Supplementary material: An Elastic Basis for Spectral Shape Correspondence

Florine Hartwig
florine.hartwig@uni-bonn.de
University of Bonn
Bonn, Germany

Josua Sassen
josua.sassen@uni-bonn.de
University of Bonn
Bonn, Germany

Omri Azencot
azencot@cs.bgu.ac.il
Ben Gurion University of the Negev
Beer Sheva, Israel

Martin Rumpf
martin.rumpf@uni-bonn.de
University of Bonn
Bonn, Germany

Mirela Ben-Chen
mirela@cs.technion.ac.il
Technion - Israel Institute of Technology
Haifa, Israel

ACM Reference Format:
Florine Hartwig, Josua Sassen, Omri Azencot, Martin Rumpf, and Mirela Ben-Chen. 2023. Supplementary material: An Elastic Basis for Spectral Shape Correspondence. In *Special Interest Group on Computer Graphics and Interactive Techniques Conference Conference Proceedings (SIGGRAPH '23 Conference Proceedings), August 6–10, 2023, Los Angeles, CA, USA*. ACM, New York, NY, USA, 4 pages. https://doi.org/10.1145/3588432.3591518

1 TECHNICAL COMPUTATIONS

1.1 Proofs of Lemmata

Lemma 1. *Let $F \in \mathbb{R}^{n,m}$ with $n, m > 0$ be a linear operator between two finite-dimensional Hilbert Spaces and $|||\cdot|||$ the corresponding Hilbert–Schmidt norm then*

a) *for all injective $\Phi_k \in \mathbb{R}^{n,k}$, $k > 0$*

$$|||F|||^2 = \left\|\Phi_k \Phi_k^\dagger F\right\|^2 + \left\|\left(I - \Phi_k \Phi_k^\dagger\right) F\right\|^2$$

b) *and for all injective $\Phi_k \in \mathbb{R}^{m,k}$, $k > 0$*

$$|||F|||^2 = \left\|F\Phi_k \Phi_k^\dagger\right\|^2 + \left\|F\left(I - \Phi_k \Phi_k^\dagger\right)\right\|^2 .$$

Proof. Considering an injective $\Phi_k \in \mathbb{R}^{n,k}$, we define $P := \Phi_k \Phi_k^\dagger \in \mathbb{R}^{n,n}$. We use $P^2 = P$ and $P^* = P$. This holds because $\Phi_k^\dagger$ is an orthogonal projection with respect to the scalar product. For an explicit calculation, see Lemma 3. We have

$$|||PF|||^2 = \mathrm{tr}((PF)^*\, PF) = \mathrm{tr}(F^* PPF) = \mathrm{tr}(F^* PF)$$

and similar

$$\left|\left|\left| (I-P)\, F \right|\right|\right|^2 = \mathrm{tr}(F^*\,(I-P)\,(I-P)\,F) \quad = \mathrm{tr}(F^*\,(I-P)\,F)\,.$$

Using the additivity of the trace, we arrive at the statement a). Statement b) follows similarly using the invariance under cyclic permutations of the trace. □

SIGGRAPH '23 Conference Proceedings, August 6–10, 2023, Los Angeles, CA, USA

ACM ISBN 979-8-4007-0159-7/23/08.
https://doi.org/10.1145/3588432.3591518

Statement b) is an orthogonal splitting of the source space of the operator F. For this to hold, it is important to consider the Hilbert–Schmidt norm. A weighted Frobenius norm would only reflect the correct scalar product on the target space.

Lemma 2. *Let $X \in \mathbb{R}^{m,k}, Y \in \mathbb{R}^{n,k}$ be linear operators between finite-dimensional Hilbert spaces with scalar products $G_1 \in \mathbb{R}^{k,k}$ and $G_2 \in \mathbb{R}^{n,n}$.*

a) *if G_2 is diagonal the minimization $\underset{\Pi\in\mathbf{\Pi}}{\operatorname{argmin}} \left|\left|\left|\Pi^\mathrm{T} X - Y\right|\right|\right|^2$ is row separable,*

b) *if $A \in \mathbb{R}^{n,n}$ is a positive definite diagonal matrix and G_2 is diagonal the minimization $\underset{\Pi\in\mathbf{\Pi}}{\operatorname{argmin}} \left|\left|\left|X^\mathrm{T}\Pi A - Y^\mathrm{T}\right|\right|\right|^2$ is column separable.*

To obtain Lemma 4.2 in the main text, we set $X = \Phi_{2,k} C_{12}^*$, $Y = \Phi_{1,k}$, $G_1 = M_{1,k}$, and $G_2 = M_1$ and apply statement a). Similarly, we set $X^\mathrm{T} = C_{12}\Phi_{2,k}^\dagger M_2^{-1}$, $Y^\mathrm{T} = \Phi_{1,k}^\dagger$, $G_1 = M_{1,k}$, and $G_2 = A = M_1$ and apply statement b) to obtain the corresponding statement in Section 4.3 in the main text on the dual perspective.

Proof. We first relate the Hilbert–Schmidt norm $|||F|||^2$ of a general operator F between finite-dimensional Hilbert spaces with scalar products G and $\tilde{G}$, respectively, to the usual Frobenius norm $\|\cdot\|_2$. This reads as

$$\begin{aligned} |||F|||^2 &:= \mathrm{tr}(G^{-1}F^\mathrm{T}\tilde{G}F) \\ &= \mathrm{tr}(\sqrt{G^{-1}}F^\mathrm{T}\sqrt{\tilde{G}}\sqrt{\tilde{G}}F\sqrt{G^{-1}}) \\ &= \left\|\sqrt{\tilde{G}}F\sqrt{G^{-1}}\right\|_2^2, \end{aligned}$$

where $\sqrt{B}$ denotes the square root of positive-definite matrices B.

Applying this to the minimization in a), we can rewrite it as

$$\underset{\Pi\in\mathbf{\Pi}}{\operatorname{argmin}} \left\|\sqrt{G_2}\left(\Pi^\mathrm{T} X\sqrt{G_1^{-1}} - Y\sqrt{G_1^{-1}}\right)\right\|_2^2$$

As $\Pi \in \mathbf{\Pi}$, we have that each column of $\Pi \in \{0,1\}^{m,n}$ has exactly one non-zero entry. Hence, $\Pi^\mathrm{T} X$ is a row permutation of X. As G_2 is diagonal by assumption, the factor $\sqrt{G_2}$ is weighting the matrices row-wise and can be omitted. The minimization can then be solved row-wise by setting $\Pi(i,j) = 1$ if and only if

$$i = \underset{r\in\{1,\dots,m\}}{\operatorname{argmin}} \left| \sqrt{G_1^{-1}} \left(X^{\mathrm{T}} e_r - Y^{\mathrm{T}} e_j \right) \right|_2^2$$

for all $j = 1, \dots, n$, which is the same as

$$i = \underset{r\in\{1,\dots,m\}}{\operatorname{argmin}} \left| G_1^{-1} \left(X^{\mathrm{T}} e_r - Y^{\mathrm{T}} e_j \right) \right|_{G_1}^2 .$$

For statement b), we rewrite the minimization as

$$\underset{\Pi\in\Pi}{\operatorname{argmin}} \left\| \sqrt{G_1} \left(X^{\mathrm{T}} \Pi A - Y^{\mathrm{T}} \right) \sqrt{G_2^{-1}} \right\|_2^2$$

Now, $X\Pi$ is a permutation of the columns of X. As $\sqrt{G_2}$ and A^{-1} are diagonal and multiplication from the right is weighting the columns, we can solve the minimization by setting $\Pi(i,j) = 1$ if and only if

$$i = \underset{r\in\{1,\dots,m\}}{\operatorname{argmin}} \left| \sqrt{G_1} \left(X^{\mathrm{T}} e_r - Y^{\mathrm{T}} A^{-1} e_j \right) \right|_2^2$$

for all $j = 1, \dots, n$. □

Lemma 3 (Orthogonal projection). *The operator $\Phi_k \Phi_k^\dagger \in \mathbb{R}^{n,n}$ is self-adjoint for an injective $\Phi_k \in \mathbb{R}^{n,k}$ with $n > k > 0$, i.e. it holds $\left(\Phi_k \Phi_k^\dagger\right)^* = \Phi_k \Phi_k^\dagger$.*

Proof. Let us recall the definition $\Phi_k^\dagger = G_k^{-1} \Phi_k^{\mathrm{T}} G$ with $G_k = \Phi_k^{\mathrm{T}} G \Phi_k$, where $G \in \mathbb{R}^{n,n}$ represents the scalar product of the Hilbert space. We have

$$\left(\Phi_k \Phi_k^\dagger\right)^* = G^{-1} (\Phi_k^\dagger)^{\mathrm{T}} \Phi_k^{\mathrm{T}} G = G_k^{-1} G_k \Phi_k G_k^{-1} \Phi_k^{\mathrm{T}} G = \Phi_k \Phi_k^\dagger$$

□

1.2 Computation of the adjoint

Computation of the adjoint (Formula (7))

$$\begin{aligned} C_{12}^* &= M_{2,k}^{-1} \Phi_{2,k}^{\mathrm{T}} P_{12}^{\mathrm{T}} (\Phi_{1,k}^\dagger)^{\mathrm{T}} M_{1,k} \\ &= \left(M_{2,k}^{-1} \Phi_{2,k}^{\mathrm{T}} M_2 \right) M_2^{-1} P_{12}^{\mathrm{T}} (\Phi_{1,k}^\dagger)^{\mathrm{T}} M_{1,k} \\ &= \left(M_{2,k}^{-1} \Phi_{2,k}^{\mathrm{T}} M_2 \right) \left(M_2^{-1} P_{12}^{\mathrm{T}} M_1 \right) \Phi_{1,k} M_{1,k}^{-1} M_{1,k} = \Phi_{2,k}^\dagger P_{12}^* \Phi_{1,k} , \end{aligned}$$

where we used $(\Phi_{1,k}^\dagger)^{\mathrm{T}} = M_1 \Phi_{1,k} M_{1,k}^{-1}$.

2 ADDITIONAL VISUALIZATION

2.1 Additional qualitative results

In Figure 1 we give additional qualitative results for the remaining methods in Figure 5 of the main paper, see Section 5.1 for details. In Figure 2 we show a colormap representation for the experiment described in Section 5.2 of the main document. Moreover, we show the results for a shape pair with median error of our method in Figure 3. In this example the extrinsic features of the shapes vary strongly.

Table 1: Runtime report (in sec).

model (number vertices)	LB basis	Ours
Cat Lion (ca. 6k)	2.82/66.74	33.59/87.96
Homer (ca. 6.5k)	1.53/24.06	22.96/33.29
Head (ca. 15k)	2.31/42.29	38.28/131.88

2.2 Qualitative results for different values of k

We show qualitative results for the iterative process initialized by a ground-truth vertex map as described in 5.4.2 in the main paper in Figure 4.

2.3 Runtime analysis

We report runtime values in Table 1 for the experiments of the main document shown in Figures 5 and 6. We distinguish between the computation of the basis functions (first value) and the iterative method (second value).

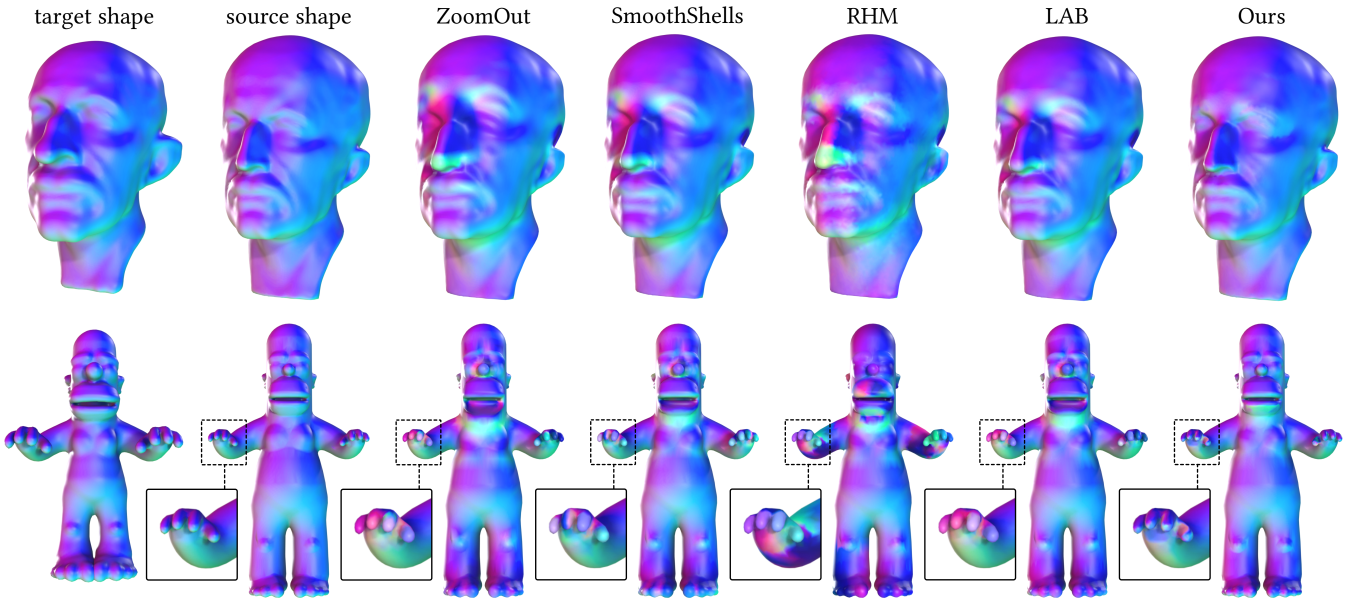

Figure 1: Additional qualitative results for Figure 5 of the main paper. See Section 5.1 in main paper for details and Figure 5 of the main paper for a quantitative evaluation of these results.

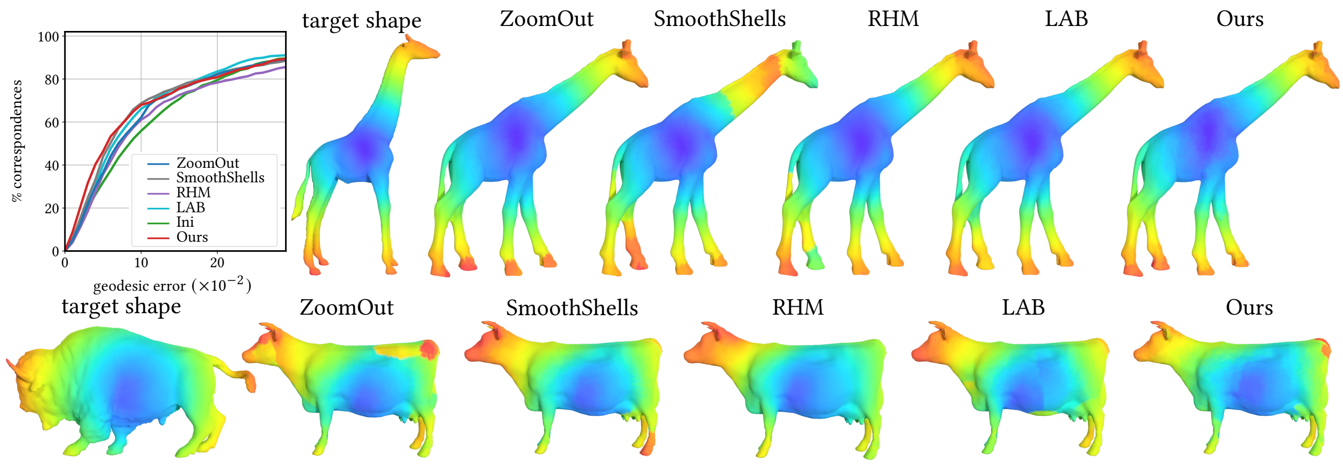

Figure 2: Colormap representation of the results of Figure 8 in the main paper.

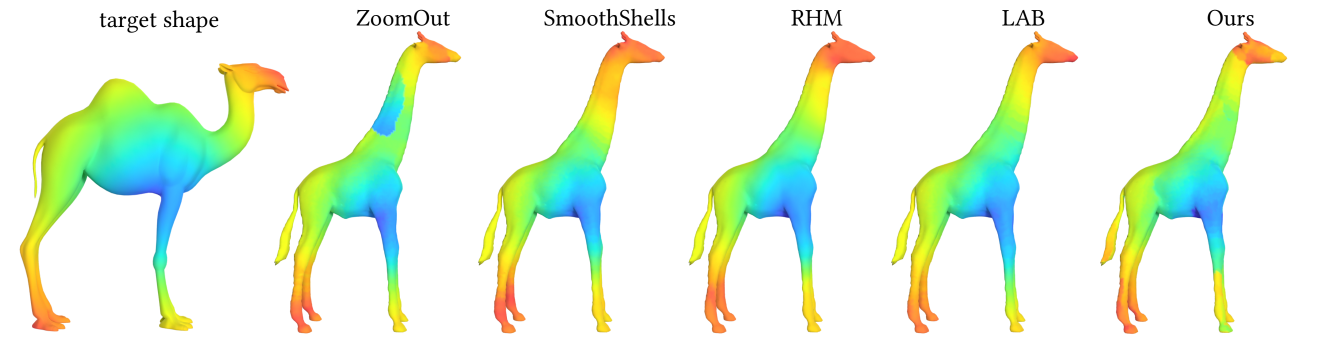

Figure 3: Correspondence of Shrec20 with median error of our method, see Section 5.4.2 for details.

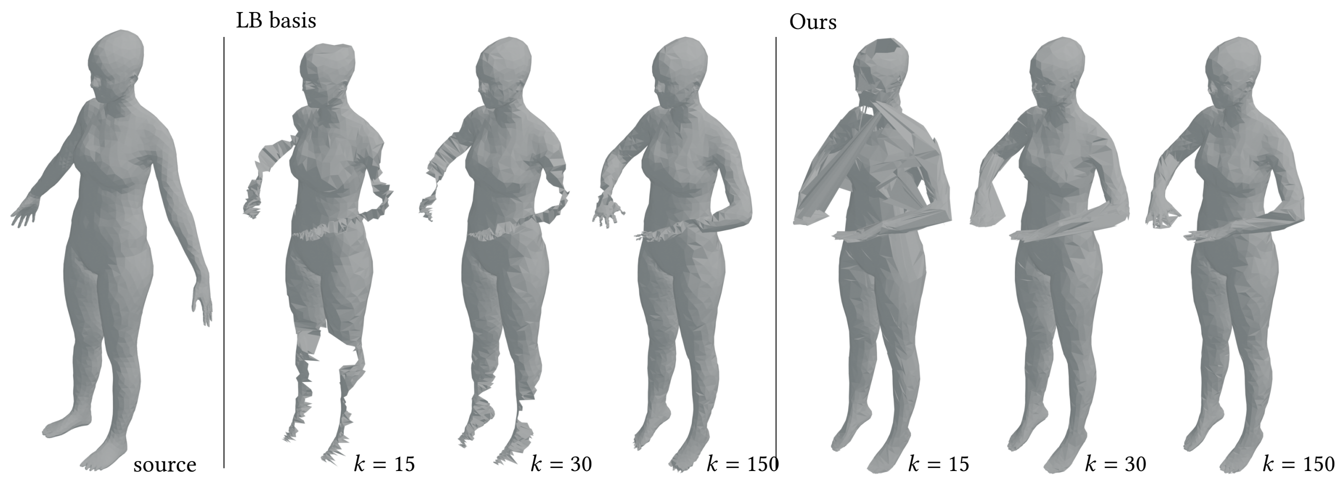

Figure 4: Qualitative visualization of results of one correspondence for different values of k for the experiment in Figure 10 of the main paper. We visualize the computed correspondence by showing the image of the resulting vertex map.